

# Neuronal Differentiation of Embryonic Stem Cell Derived Neuronal Progenitors Can Be Regulated by Stretchable Conducting Polymers

Nishit Srivastava, MS,<sup>1</sup> Vijay Venugopalan, MSc,<sup>1</sup> M.S. Divya, MSc,<sup>2</sup> V.A. Rasheed, MSc,<sup>2</sup> Jackson James, PhD,<sup>2</sup> and K.S. Narayan, PhD<sup>1</sup>

Electrically conducting polymers are prospective candidates as active substrates for the development of neuroprosthetic devices. The utility of these substrates for promoting differentiation of embryonic stem cells paves viable routes for regenerative medicine. Here, we have tuned the electrical and mechanical cues provided to the embryonic stem cells during differentiation by precisely straining the conducting polymer (CP) coated, elastomeric-substrate. Upon straining the substrates, the neural differentiation pattern occurs in form of aggregates, accompanied by a gradient where substrate interface reveals a higher degree of differentiation. The CP domains align under linear stress along with the formation of local defect patterns leading to disruption of actin cytoskeleton of cells, and can provide a mechano-transductive basis for the observed changes in the differentiation. Our results demonstrate that along with biochemical and mechanical cues, conductivity of the polymer plays a major role in cellular differentiation thereby providing another control feature to modulate the differentiation and proliferation of stem cells.

## Introduction

IT IS WELL KNOWN that cells anchor on substrates through extra-cellular matrix proteins.<sup>1–3</sup> The formation and stabilization of focal adhesion complexes on substrates are known to be significantly influenced by local mechanical, topographical, and electrostatic environment<sup>4–9</sup> and this eventually controls various intra-cellular activities, such as cell division, migration, proliferation, and differentiation.<sup>10–17</sup> Conducting polymers (CPs) provide a unique microenvironment for proliferation and differentiation of cells.<sup>18–21</sup> The electronic and ionic characteristics of these electrochemically active polymers have been utilized in the generation of neuronal probes and biosensors.<sup>22–24</sup> The prospect of having such smart-electrode interface on flexible-stretchable substrates opens up a valuable gateway to monitor and control biological events.<sup>25</sup> In the field of regenerative medicine, the CP based microelectrodes can simultaneously act as scaffolds providing mechanical support and also provides molecular-cues for regenerating neurons.<sup>18,26,27</sup> Here we have highlighted the importance of these composite substrates for differentiation of embryonic stem cell derived neural progenitors (ES-NPs) into neurons.

The role of surface properties of the polymer on the differentiation of adult neural stem cells has been well demonstrated,<sup>28,29</sup> where an increase in the differentiation of neural stem cells on soft PDMS-type substrates is observed as opposed to harder oxide surfaces.<sup>30–32</sup> The electrostatic aspect of the surface which stem cells perceive from the extra-cellular matrix; however, has received relatively less attention. Surface charge properties of the matrix change with the interfacial mechanical properties and hence, it is important to discern its role since these properties are known to alter cell adhesion.<sup>33,34</sup> The surface charge on the substrate can alter the recruitment of proteins, which in turn influences the formation of focal adhesion complexes and lead to changes in the downstream signaling events.<sup>35,36</sup> We show that a subtle and controlled method of modifying the polymer surface is achieved by stretching. A careful study of cell differentiation on surfaces which have different degrees of strain provides a clear demonstration of the substrate effect.

The present report focuses on differentiation of mouse ES-NPs into neurons on stretched and electrified PEDOT:PSS (Poly(3,4-ethylenedioxythiophene) poly(styrenesulfonate)) coated styrene ethylene butylene styrene (SEBS) substrates. We further demonstrate the effect of electroactivity and

<sup>1</sup>Molecular Electronics Laboratory, Chemistry and Physics of Materials Unit, Jawaharlal Nehru Centre for Advanced Scientific Research, Bangalore, India.

<sup>2</sup>Neural Stem Cell Biology Lab, Neurobiology Division, Rajiv Gandhi Centre for Biotechnology, Trivandrum, India.

varying charge distribution produced due to alignment of polymer chains of the substrates upon application of strain, on the differentiation of ES-NPs. A decrease in ES-NP differentiation into neurons was observed with increased applied strain on CPs. Cell distribution was also affected by the strain applied on the substrates, as indicated by significant fraction of the differentiated neurons taking the form of aggregates. Neuronal differentiation was observed in these aggregates near the surface of polymer thereby showing the strong guiding tendency of polymeric surface for the differentiation of ES-NPs. Studies to resolve and deconvolute the effect of mechanical cues from the electrical parameters of the substrate in the cell distribution, cytoskeletal organization, and differentiation of ES-NPs were also carried out.

## Materials and Methods

### *Preparation of SEBS/PEDOT:PSS substrates*

SEBS (KRATON 1726-G) was processed with chloroform as solvent to form thin stretchable films of SEBS (~400  $\mu\text{m}$ ). Subsequently,  $1 \times 1.2$  cm rectangular substrates were cut and plasma treated for 2 min, at 0.5 bar pressure and 0.08 A current. The aqueous dispersion of PEDOT:PSS (Agfa, Orgacon Printing Ink EL-P3040) was spin coated on SEBS substrates at 2500 rpm for 60 s to obtain films of ~90 nm thickness which were annealed at 65°C for 12 h.<sup>37</sup> The setup for straining the PEDOT:PSS coated SEBS substrates was a homebuilt setup with a calibrated screw gauge. Substrates were strained by clamping at the two ends and were uniaxially strained to different strain regimes of 10%, 20%, 30%, and 5 cycles of 30% strain (Supplementary Fig. S1; Supplementary Data are available online at [www.liebertpub.com/tea](http://www.liebertpub.com/tea)). The strained conducting substrates were maintained in stretched condition by wedging them cleanly to a glass slide of the same dimension using araldite. The pristine SEBS substrates were prepared in the similar manner following the similar procedure barring the coating with CP PEDOT:PSS. Detailed information about the substrate preparation is available in supplementary information.

### *Characterization of substrates*

AFM study of the substrates was done in contact mode using a JPK instruments Nanowizard 3 Nanoscience AFM. Kelvin probe microscopy (KPM) was also done in contact mode and amplitude of 0.1 V was applied during scanning.

### *Embryonic stem cell culture and ES-NP generation*

Embryonic stem cell culture and EB induction was done by established standard protocol.<sup>38</sup> Briefly, mouse D3 ES cells (ATCC) were cultured on gelatin substrate in embryonic stem cell growth medium (ESGM) consisting of DMEM, 10% defined fetal bovine serum (FBS), 2 mM L-glutamine,  $1 \times$  nucleosides, 0.1 mM  $\beta$ -mercaptoethanol, and 1000 U/mL leukemia inhibitory factor (LIF). EBs were generated by growing ES cells on uncoated plates in EB medium (ESGM without LIF and  $\beta$ -mercaptoethanol) for 4 days and with EB medium containing 0.5  $\mu\text{M}$  retinoic acid (RA) for an additional 4 days. RA induced EBs were partially differentiated on poly-D-lysine (150  $\mu\text{g}/\text{mL}$ ) and laminin (1  $\mu\text{g}/\text{mL}$ ) coated substrate for 2 days in N2 differentiation medium (DMEM/F12) supplemented with 1% N2 supplement, FGF2 (10 ng/

mL), or epidermal growth factor (EGF) (10 ng/mL), heparin (2  $\mu\text{g}/\text{mL}$ ), and 0.5% FBS.<sup>39</sup> The partially differentiated EBs were trypsinized mildly and plated onto uncoated six-well plates (~ $1.5 \times 10^6$  cells/well) in proliferation medium consisting of DMEM/F12 supplemented with 1% N2 supplement, heparin (2  $\mu\text{g}/\text{mL}$ ), and FGF2 (20 ng/mL) and allowed to proliferate further for 4 days.

ES-NPs were differentiated on polymer substrates pretreated with PDL and laminin. N2 differentiation medium was used to differentiate the ES-NPs on the substrates. After 8–10 days of differentiation, cells were fixed for immunofluorescence analysis. Further, to demonstrate that the differentiated cells are indeed physiologically active neurons, we differentiated GAD65-EGFP expressing ES cells with the above differentiation conditions. GAD65 is an enzyme that is responsible for conversion of glutamate into GABA at the synaptic terminals of physiologically active neurons.<sup>40</sup> In addition to this, specific localization of synaptotagmin at the synapse was checked to confirm that the cells differentiated from ES-NPs are indeed neurons.<sup>41</sup>

### *Immunofluorescence analysis*

Immunofluorescence analysis was carried out for detection of cell specific markers.<sup>39</sup> Briefly, 4% paraformaldehyde-fixed cells were blocked in 5% NGS (Sigma-Aldrich) and permeabilized with 0.2%–0.4% Triton-X 100 followed by an overnight incubation with primary antibodies at 4°C ( $\beta$ -III tubulin 1:200 Chemicon, GFAP 1:400 Sigma). Cells were examined for fluorescence after incubation with appropriate secondary antibody conjugated to FITC (1:400) or cy3 (1:400). Actin cytoskeleton of differentiated cells were observed by FITC conjugated Phalloidin (1:750; Molecular Probes). Nuclear staining was done with DAPI (1:50000) and used for counting total number of cells. An upright fluorescence microscope with cooled CCD camera (Olympus BX-61) was used for capturing images under 20 $\times$  objective. Confocal imaging was done using Zeiss LSM 510 Meta microscope.

Cell counting was done from the acquired immunostained images of neuronal and glial cells. Briefly, 7–8 fields of each polymeric substrate were imaged, and the number of  $\beta$ -III tubulin positive and GFAP positive cells were obtained by manual counting of the merged images. Cells stained with nuclear stain DAPI were used for counting the total number of cells. One-way analysis of variance was performed in all the statistical analysis using Origin and significance was depicted at  $p < 0.05$ . Neurite length was measured by Simple Neurite Tracer plug-in of the Image J software.<sup>42,43</sup> The area of the aggregates was measured by binarizing the DAPI images of the differentiated cells on the substrates by Image J software.<sup>43,44</sup>

## Results

### *Properties of conducting substrates change on application of strain*

Conducting polymeric substrates were fabricated by coating PEDOT:PSS (a CP with anionic surfactant PSS as a counter-ion) over an elastomer SEBS. Application of strain increases the surface conductance of the PEDOT:PSS coated SEBS substrates in a manner similar to our previous results.<sup>37</sup> AFM images of the substrates revealed the changes in

nanotopographical features of CP-coated SEBS substrates with the application of strain (Supplementary Fig. S2).

KPM analysis provided the distribution of surface potential on conducting substrates (Fig. 1A, B). PEDOT rich clusters which are arranged in the form of circular domains in the PSS matrix, redistribute along the strain direction when elongated, leading to a change in the distribution of surface potential on these conducting substrates (Fig. 1B). Contact angle measurement of the substrates showed that the application of strain does not alter the hydrophobicity of the substrates (Supplementary Fig. S3).

#### CPs influence the neuronal differentiation potential of ES-NPs

ES-NPs were seeded onto PEDOT:PSS coated SEBS substrates and SEBS with and without straining (Supplementary Fig. S4). The glass-coverslips and PEDOT:PSS coated glass coverslips were used as controls in the experiment. In general ES-NPs differentiated into neuronal cells, as evident from the uniform presence of  $\beta$ -III tubulin<sup>+ve</sup> cells on the entire surface of substrates even though there was a marked difference in gross morphology of the differentiating neurons (Fig. 2 and Supplementary Figs. S5–S8). To further confirm the neuronal identity of the differentiated cells, we have differentiated GAD65-EGFP expressing ES cells on glass coverslips. The presence of GABA in the inter-linking neuronal network clearly indicates that they are active synaptic terminals which can be present only in physiologically active neurons. Therefore, it is clear that these differentiated neurons are capable of forming interlinking networks amongst them (Supplementary Fig. S9).

The differentiation of neurons enhances with increased straining of nonconducting pristine SEBS-substrates and formed a monolayer of differentiated neurons (Fig. 2B–D). Neuronal differentiation occurred with the formation of aggregate-like structures on the strained CP-coated SEBS substrate. The neurons present within the aggregates formed interlinking neuronal-networks which extended to neighboring aggregates (Fig. 2F–H).

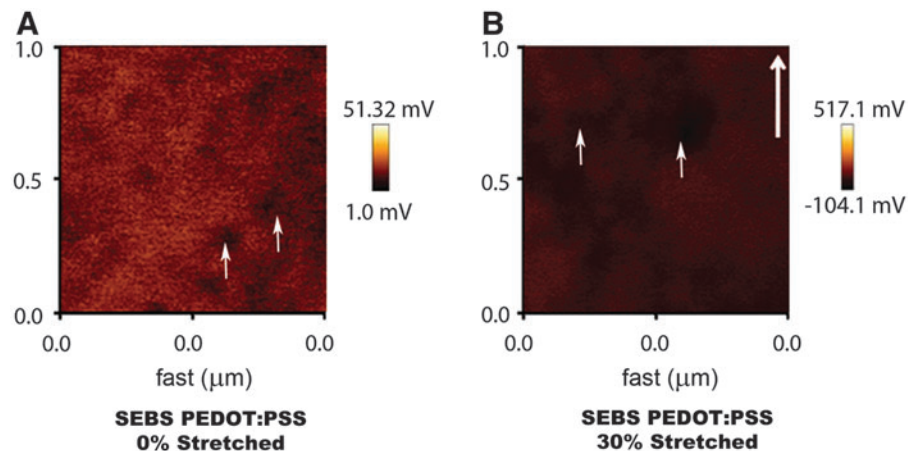
The total aggregate size was measured by binarizing the DAPI image which gave the surface area covered by the nucleus of all the cell types present within the aggregates. The surface area of the aggregates also increased with an increase in

the applied strain (Fig. 2F–H). On unstrained CP substrates, the cellular aggregates had an average size of  $12,020 \pm 3203 \mu\text{m}^2$  in terms of their nuclear area, whereas on highly strained (30%) CP substrates the average nuclear surface area of aggregates increased to  $85,285 \pm 9728 \mu\text{m}^2$  (Fig. 2I). The average nuclear surface area of the aggregates formed on SEBS substrates were found to be generally low with  $9367 \pm 802 \mu\text{m}^2$  for unstrained SEBS substrates as compared to  $3504 \pm 907 \mu\text{m}^2$  in case of 30% strained pristine SEBS substrates.

We further analyzed other parameters of neuronal differentiation, such as the percentage of differentiated neurons and the neurite length on CP-coated as well as SEBS controls. The percentage of  $\beta$ -III tubulin<sup>+ve</sup> cells decreased with increase in strain regime on PEDOT:PSS coated substrate compared to SEBS (Fig. 3A). Differentiation of ES-NPs on 30% strained PEDOT:PSS coated substrates resulted in a significant reduction of neuronal differentiation compared to unstrained (0%) PEDOT:PSS coated substrates ( $11.8\% \pm 1.8\%$  and  $26.7\% \pm 2.5\%$ , respectively;  $p < 0.05$ ). We also found a significant increase in the neuronal differentiation on strained (30%) pristine SEBS substrates compared to similarly strained CP-coated substrates ( $36.2\% \pm 1.2\%$  and  $11.8\% \pm 1.8\%$ , respectively) ( $p < 0.05$ ). Another interesting observation was the difference in length of neurites. Neurite length (NL) was measured using an imaging-software where only surface-neurons were sampled and the possibility of three-dimensional growth and extension deep into the aggregate were not considered. The differentiated neurons on unstrained (0%) PEDOT:PSS coated substrates had significantly longer neurites ( $115.5 \pm 4.7 \mu\text{m}$ ) compared to highly strained (30%) substrates ( $41.7 \pm 2.6 \mu\text{m}$ , Fig. 3B). In contrast to this, average NL of differentiated neurons on SEBS-substrates were found to be proportionate to the strain, with NL extending from ( $145.7 \pm 9.1 \mu\text{m}$ ) for unstrained SEBS to ( $215.5 \pm 5.6 \mu\text{m}$ ) for 30% strained SEBS.

The formation of aggregates during the differentiation process is clearly correlated to the presence of conducting layer. Therefore, we further probed the aggregated cells present at the substrate-cell interface using confocal microscopy. The substrate-cell interface is the region where the cells come directly in contact with the substrate. Confocal imaging of the differentiated cellular aggregates showed that the neuronal differentiation occurred at all the strata of the aggregates (Fig. 4A, B). It was also observed that the number of

**FIG. 1.** Kelvin probe microscopy (KPM) image showing variation in the surface potential of (A) SEBS PEDOT:PSS 0% Stretched (B) SEBS PEDOT:PSS 30% Stretched substrates. Bold arrow indicates the direction of strain, while small arrows indicate the PEDOT domains. The alignment and distribution of PEDOT domains change on straining the substrates. SEBS, styrene ethylene butylene styrene; PEDOT:PSS, (poly(3,4-ethylenedioxythiophene) poly(styrene sulfonate)). Color images available online at [www.liebertpub.com/tea](http://www.liebertpub.com/tea)



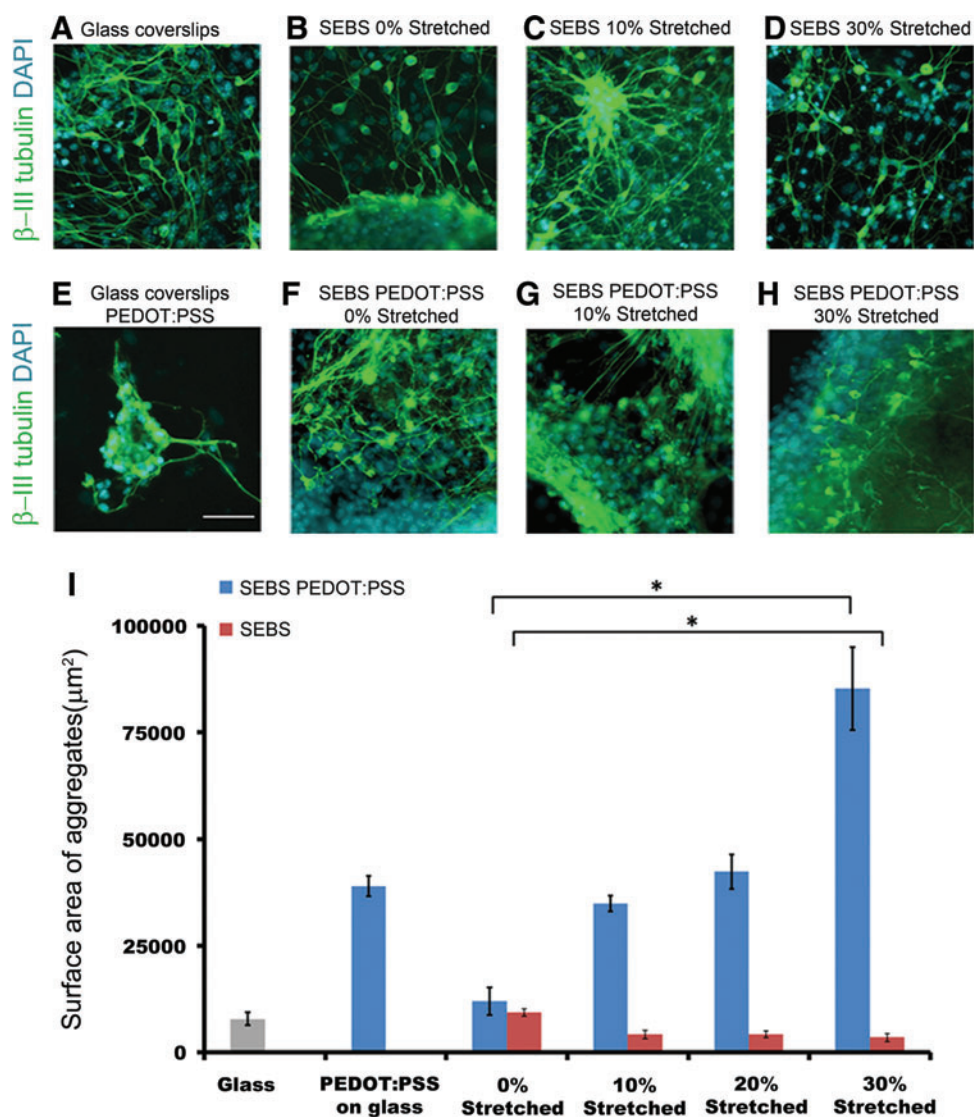


**FIG. 2.** Immunocytochemistry for differentiation of ES-NPs into neurons ( $\beta$ -III tubulin) on (B–D) SEBS, (F–H) PEDOT:PSS coated SEBS substrates and (A, E) glass coverslips and PEDOT:PSS coated glass coverslips (control). (I) Distribution of the surface area of the cell aggregates (nuclear) formed on each substrate ( $*p < 0.05$ , One-way analysis of variance (ANOVA)). Data are represented as mean  $\pm$  SD,  $n = 3$ . (A–H): Scale bar 50  $\mu$ m. Color images available online at [www.liebertpub.com/tea](http://www.liebertpub.com/tea)

differentiated cells was more at the substrate-cell interface than at the upper half of the aggregates (Fig. 4B). The neurons present at the top region of these aggregates exhibited much shorter neurites with very little branching. At the substrate-cell interface, neurons formed well defined network of interconnected neurites with a decrease in neurite length as the function of distance from the substrate (Fig. 4A). Populations of differentiated neurons were present within the aggregate on strained CP-substrates and were comparable with their nonconducting strained counterparts.

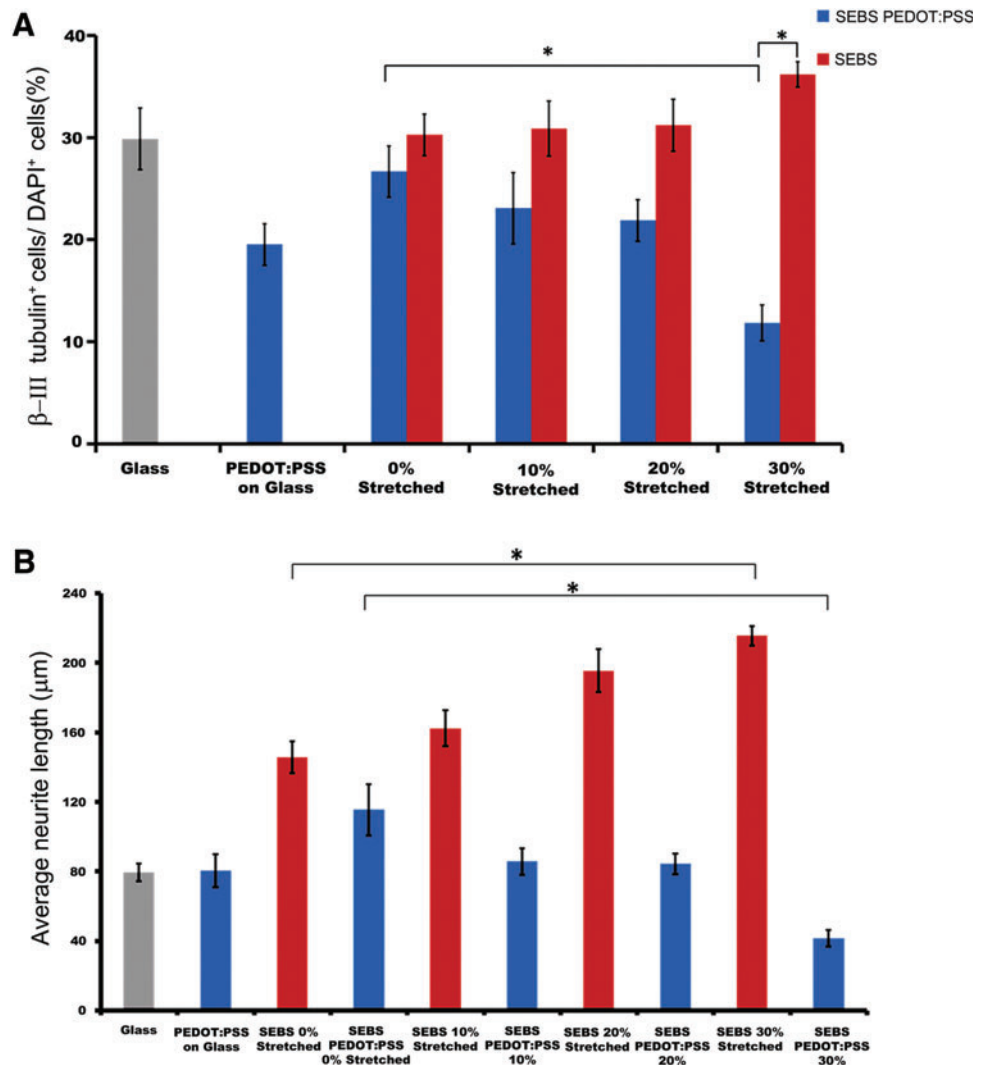
Glial differentiation was also analyzed using GFAP staining and significant change in their differentiation was not observed upon straining the conducting substrate (Supplementary Fig. S10 A–I).

#### *Neurons tend to follow the cues from local defect patterns produced by stretching the CPs*

Even though the surface texture and film quality is maintained at the micrometer level, the strained bilayer-

substrates are expected to have crack-type defects which emerge orthogonal to the strain direction. The appearance of crevices on the top conducting layer of the strained films can dock and immobilize the cell aggregates.<sup>45</sup> The jagged crack edges can possibly offer the cell aggregates a preferred direction, which is indicated by the ellipsoidal geometry of the aggregates where the long axis is largely distributed within an angle of 20° orthogonal to the strain (Fig. 5A–F and Supplementary Figs. S11 and S12). This viewpoint is consistent with the observation on 30% strained CP substrates where 70.2%  $\pm$  5.3% of aggregates were aligned along these local defects in contrast to only 21.9%  $\pm$  4% aggregates being aligned on nonconducting SEBS substrates strained to similar regime ( $p < 0.05$ ; Fig. 5G). The alignment of aggregates along the defects decreased sharply for substrates which were exposed to a lower strain magnitude. 39.8%  $\pm$  6.4% of aggregates were aligned along the defect patterns on 20% strained CP substrates, while no significant alignment was observed on the corresponding nonconducting strained SEBS counterparts.

**FIG. 3.** Substrate dependence of neuronal differentiation and average neurite length. Neurite length was measured by Image J software and only those neurons were considered for sampling which were spread out on the substrates. **(A)** Distribution of the percentage of  $\beta$ -III tubulin positive cells on various substrates ( $*p < 0.05$ , One-way ANOVA). **(B)** Distribution of the average neurite length of the neurons on various substrates ( $*p < 0.05$ , One-way ANOVA). Data are presented as mean  $\pm$  SD, ( $n = 3$ ). Color images available online at [www.liebertpub.com/tea](http://www.liebertpub.com/tea)



### Rearrangement of Actin-based cytoskeleton

Arrangement of actin cytoskeleton was observed by staining the differentiated ES-NPs with phalloidin (Fig. 6A–F and Supplementary Fig. S13). Aggregated cells on the CP surface revealed disruption in the arrangement of actin fibers, while the differentiated neurons on nonconducting pristine SEBS substrates and control glass-coverslips exhibited well-arranged actin fibers. A similar feature was also seen on the patterned SEBS/PEDOT:PSS substrates where the differentiated cells adopted a circular morphology with a disrupted actin fiber network on the conducting side of this substrate. Neurons which originated from the nonconducting SEBS side were seen to be abruptly terminated at the conducting/nonconducting interface. Actin fibers were uniformly arranged on the nonconducting SEBS side leading to a better neuronal distribution and differentiation. Along with neurons, other cell types like fibroblasts, which differentiated from ES-NPs, also exhibited disruption of actin fibers and had a tendency to circularize on the conducting side of the substrate.

### Discussion

In general, our observations point towards trends which indicate that the neuronal differentiation of ES-NPs is

controllable, by tuning the local electrostatics and mechanical factors. The surface conductance and the morphology of the CP substrates are varied by the application of increasing strain regime. The randomly distributed spherical PEDOT domains transform into ellipsoidal domains within the anionic PSS matrix.<sup>46</sup> The remodeling of PEDOT domains contribute to the changes in the surface potential distribution of CP substrates, suggesting a control in distribution of these surface potentials at nanometer length scales by straining (Fig. 1A, B).

Application of strain also leads to the variation in the neuronal differentiation potential of ES-NPs on conducting as well as nonconducting substrates. A decrease in the neuronal differentiation was observed along with an inhibition in cell spreading on the strained CP-substrates, forcing the cells to grow within the aggregates (Figs. 2A–I and 3A). The shorter length of neurites on the surface of strained CP substrates can be attributed to the presence of varying surface potential regions and local defects which affect the cell attachment and also impede the neurite elongation (Fig. 3B). Confocal scanning of the cellular aggregates on CP-substrates showed that the differentiation occurred in all the strata of the aggregates but the morphology of neurons spread on the substrate was distinct from these neurons (Fig.

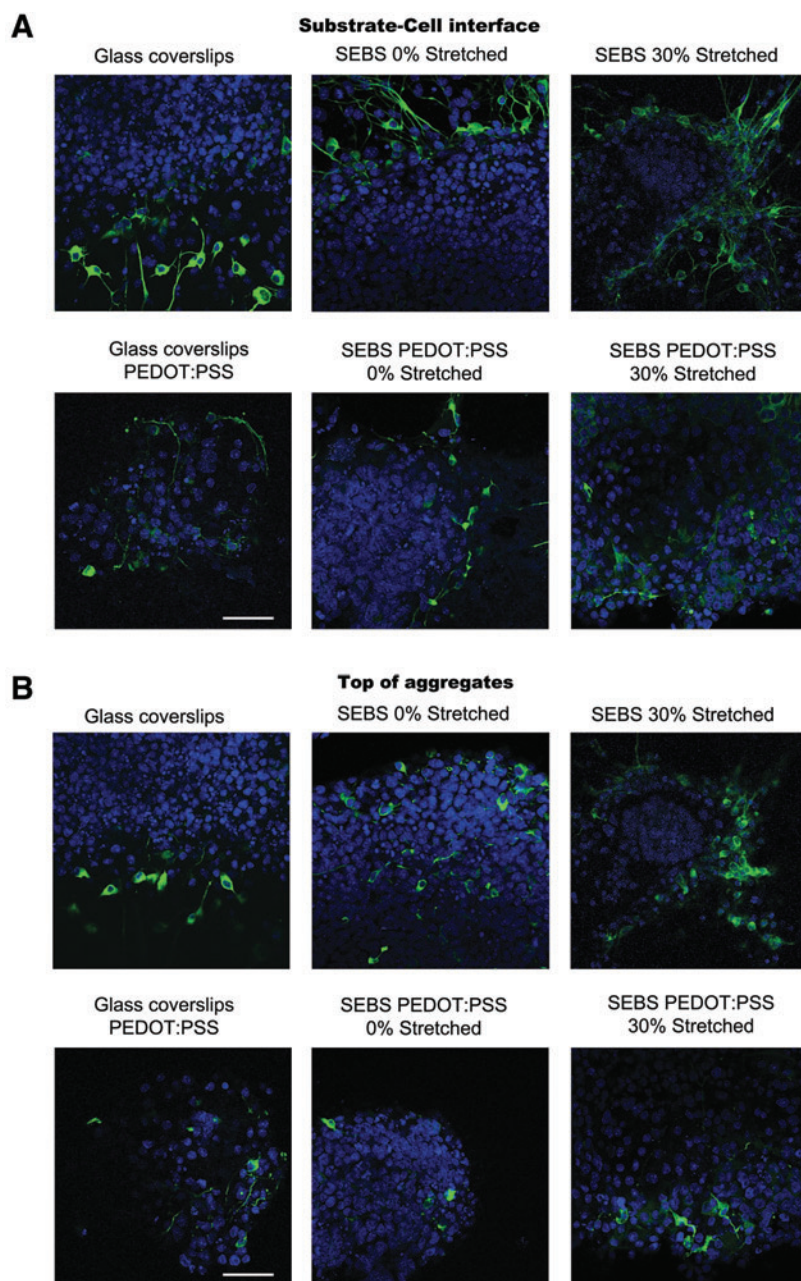


**FIG. 4.** Confocal image of cell aggregate density with focal plane at **(A)**  $z=0$  corresponding to the substrate-cell interface **(B)** Top of the cell aggregate. Neuronal differentiation occurs at all the strata of the aggregates with extensive neurite branching on strained CP substrates. Scale bar, 50  $\mu\text{m}$ . Color images available online at [www.liebertpub.com/tea](http://www.liebertpub.com/tea)

4A, B). The neurons differentiating in the close proximity of the polymer surface had a characteristic shape of a neuronal cell, while those at a distance were less spread and extended fewer neurites. These changes corroborate the possible role of polymeric substrate for the physical guidance during differentiation of ES-NPs. Cell adhesion on CP substrates is primarily attributed to the adsorption of extra-cellular matrix proteins like laminin on the surface of the substrate.<sup>35</sup> The changes in the local electrostatics of the substrate may lead to the differential adsorption of these ECM which affects the cell adhesion and formation of stable focal adhesion complexes.

As discussed earlier, application of strain on the substrates also leads to the generation of slip defects on CP-coated substrates due to delamination of PEDOT:PSS film resulting

in a local defect pattern due to which underlying SEBS surface is exposed. The “crack patterning” of the aggregates along these jagged edges is solely due to the defects formed in the PEDOT:PSS layer on SEBS which yields easily to allow the generation of these defects, while SEBS surface, in comparison, maintains its texture at such strain levels.

The changes in the cytoskeleton arrangement of the differentiated ES-NPs were investigated on polymeric substrates, primarily to understand the variations occurring within the cells on these substrates (Fig. 6A–F). The CP-coated substrates, where cells tend to aggregate, exhibited disruption of actin fibers, while on the control glass-coverslips or SEBS substrates, the actin fibers were arranged in an ordered fashion. These observations are in complete conjunction with the role of cytoskeletal tension in modulating

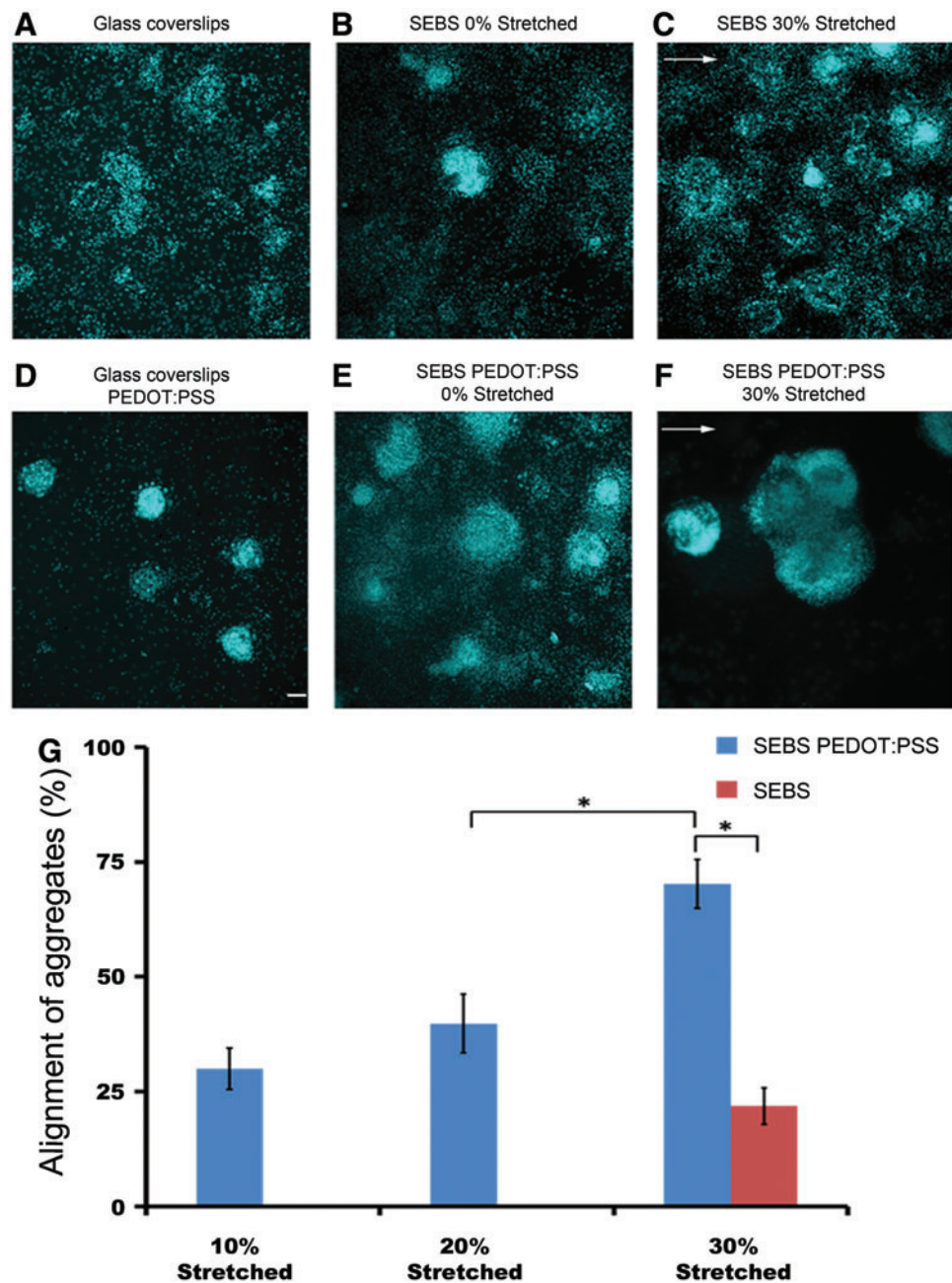


**FIG. 5.** Directional alignment of the cell aggregates along the local defects generated orthogonal to the strain direction (A–F). Arrows in the figure indicate the strain direction. (G) Distribution of the directional alignment of cellular aggregates along the “defect patterns” generated on polymeric substrates ( $*p < 0.05$ , One-way analysis of variance). Data are represented as mean  $\pm$  SD, ( $n = 3$ ). (A–F): Scale bar, 50  $\mu\text{m}$ . Color images available online at [www.liebertpub.com/tea](http://www.liebertpub.com/tea)

the differentiation, movement and growth of cells. Rho-A and ROCK signaling which modulates the stress generated by actin-myosin complex has been shown to regulate the mesenchymal stem cell differentiation into osteoblasts and chondrocytes.<sup>47</sup> The role of substrate stiffness in directing the differentiation of stem cells leading to similar changes in cytoskeletal system has also been reported.<sup>30,48</sup> The cells form focal adhesion complexes, tethered to the actin fibers, upon attachment to the substrate. The change in the actin distribution upon the attachment of the cells to the substrate modulates these focal adhesion complexes leading to changes in cellular differentiation and spreading of cells. The maturation of focal adhesion complexes is mediated by integrin clustering which recruits other down-stream signaling molecules and this process is controlled by cytoskeletal ten-

sion.<sup>49</sup> The changes in the cell shape are the potent mediator of the actin-myosin contractility which affects the stabilization of focal adhesion complexes and other down-stream signaling events triggering a mechanotransduction like response in the cells.

The initial events leading to cell adhesion on any substrate are accompanied by seeding of extra-cellular matrix proteins on which the surface receptors of the cells are bound. The confirmation, orientation, and quantity of proteins adsorbed are influenced by the surface features, roughness, and oxidation state of the polymers.<sup>35,36</sup> The alignment of PEDOT domains in the matrix of PSS and generation of local defect patterns result in the formation of regions exhibiting variability in the surface potential and conductivity which modulates the overall distribution of proteins adsorbed on

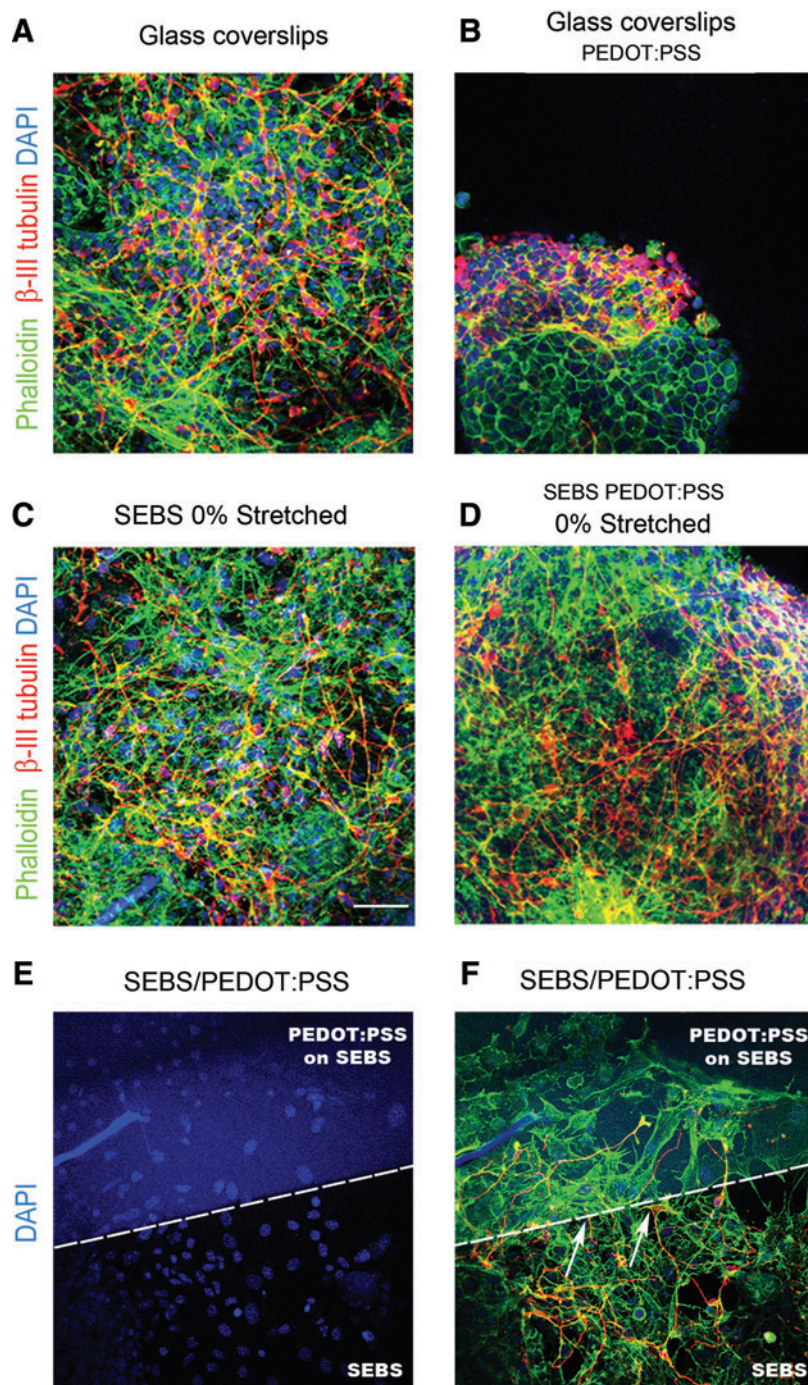


**FIG. 6.** Actin cytoskeleton (Phalloidin) of the differentiated cells on polymeric substrates (A–D, F). Regular arrangement of actin cytoskeleton is seen on (A) glass-coverslips (C) SEBS 0% stretched. Disruption of actin fibers occur on PEDOT:PSS coated SEBS substrates leading to rounded morphology and aggregation of cells (B, D). Nucleus (DAPI) of the differentiated cells on the substrate containing SEBS and PEDOT:PSS coated SEBS (E). The arrows in (F) show the neurite ending on the interface of PEDOT: PSS and SEBS. Disruption of actin cytoskeleton is also seen on the conducting side of the patterned substrate. Scale bar, 50  $\mu$ m. Color images available online at [www.liebertpub.com/tea](http://www.liebertpub.com/tea)

the CP substrates. The modulation of cell adhesion results in the variation of traction forces which the cells perceive from the substrate and it leads to the changes in the actin based cytoskeletal assembly. Initial cell adhesion events are dependent upon the favorable surface potential regions but the aggregate formation and cell spreading is influenced strongly by the underlying macroscopic film quality. On highly strained CP substrates, the distribution of surface potential is more prominent leading to confinement of cells and presence of larger defect patterns influence the cell spreading which leads to an increase in the number of cellular aggregates. The absence of conducting surface leads to

uniform surface potential regions, and this results in a different pattern of cell differentiation on nonconducting pristine SEBS controls.

Strain hardening of the SEBS leads to further increase in the stiffness of the substrates upon application of strain, the surface of elastomeric polymer SEBS is quite stiff ( $\sim 2$  MPa) in comparison to the natural environment in which neurons grow.<sup>31,50</sup> The changes in the stiff CP and pristine SEBS-substrates do not lead to large variations in the formation and maturation of focal adhesion complexes which are primary effectors of cytoskeletal arrangement and other downstream signaling events like cell adhesion and differentiation.

CP SEBS substrates allow potential development of implantable electrodes by providing a mechanical environment whose surface conductance can be modulated by application of strain. These substrates are biocompatible and provide spatial cues for directing the neuronal differentiation of ES-NPs. The polymeric substrates are quite stretchable and can be used as scaffold for the regeneration of axons in the injured tissue areas. Local defect patterning of the differentiated cells on strained CP substrates is an example of physical guidance provided by the substrate and has implications in guiding the neurites to extend along a particular direction without any chemical patterning and may have far-reaching application in designing the implants or conduits for the regeneration of axons. The flexibility of these substrates confers great advantage in the field of flexible neural implants and sensors in the human body. The modulation of actin cytoskeleton of differentiated cells by the surface conductance of the polymers and its subsequent role in regulating differentiation of ES-NPs opens up a new possibility for controlling the stem cell differentiation. However, the transduction of the effect of the electroactivity of the polymer into biochemical signals which essentially modulate the differentiation of stem cells needs to be understood at the fundamental level. The results also suggest an interesting possibility on the cellular sensing of nanodimensional conducting PEDOT domains in the insulating PSS matrix.

#### Acknowledgments

The authors acknowledge the confocal facility at JNCASR and RGCB for the help with the imaging of cells and Dr. Sanalkumar RS for generation of GAD65-EGFP cell line.

#### Disclosure Statement

No competing financial interests exist.

#### References

- Meredith, J.E., Fazeli, B., and Schwartz, M.A. The extracellular-matrix as a cell-survival factor. *Mol Biol Cell* **4**, 953, 1993.
- Colognato, H., Winkelmann, D.A., and Yurchenco, P.D. Laminin polymerization induces a receptor-cytoskeleton network. *J Cell Biol* **145**, 619, 1999.
- Gumbiner, B.M. Cell adhesion: the molecular basis of tissue architecture and morphogenesis. *Cell* **84**, 345, 1996.
- Burridge, K., Fath, K., Kelly, T., Nuckolls, G., and Turner, C. Focal adhesions: transmembrane junctions between the extracellular matrix and the cytoskeleton. *Annu Rev Cell Biol* **4**, 487, 1988.
- Dembo, M., and Wang, Y.L. Stresses at the cell-to-substrate interface during locomotion of fibroblasts. *Biophys J* **76**, 2307, 1999.
- Halliday, N.L., and Tomasek, J.J. Mechanical properties of the extracellular matrix influence fibronectin fibril assembly *in vitro*. *Exp Cell Res* **217**, 109, 1995.
- Yim, E.K.F., Darling, E.M., Kulangara, K., Guilak, F., and Leong, K.W. Nanotopography-induced changes in focal adhesions, cytoskeletal organization, and mechanical properties of human mesenchymal stem cells. *Biomaterials* **31**, 1299, 2010.
- Huebsch, N., Arany, P.R., Mao, A.S., Shvartsman, D., Ali, O.A., Bencherif, S.A., *et al.* Harnessing traction-mediated manipulation of the cell/matrix interface to control stem-cell fate. *Nat Mater* **9**, 518, 2010.
- Parekh, S.H., Chatterjee, K., Lin-Gibson, S., Moore, N.M., Cicerone, M.T., Young, M.F., *et al.* Modulus-driven differentiation of marrow stromal cells in 3D scaffolds that is independent of myosin-based cytoskeletal tension. *Biomaterials* **32**, 2256, 2011.
- Balaban, N.Q. Force and focal adhesion assembly: a close relationship studied using elastic micropatterned substrates. *Nat Cell Biol* **3**, 466, 2001.
- Beningo, K.A., Dembo, M., Kaverina, I., Small, J.V., and Wang, Y.L. Nascent focal adhesions are responsible for the generation of strong propulsive forces in migrating fibroblasts. *J Cell Biol* **153**, 881, 2001.
- Choquet, D., Felsenfeld, D.P., and Sheetz, M.P. Extracellular matrix rigidity causes strengthening of integrin-cytoskeleton linkages. *Cell* **88**, 39, 1997.
- Curtis, A., and Wilkinson, C. New depths in cell behaviour: reactions of cells to nanotopography. *Biochem Soc Symp* **65**, 15, 1999.
- Rowlands, A.S., George, P.A., and Cooper-White, J.J. Directing osteogenic and myogenic differentiation of MSCs: interplay of stiffness and adhesive ligand presentation. *Am J Physiol Cell Physiol* **295**, C1037, 2008.
- Wingate, K., Bonani, W., Tan, Y., Bryant, S.J., and Tan, W. Compressive elasticity of three-dimensional nanofiber matrix directs mesenchymal stem cell differentiation to vascular cells with endothelial or smooth muscle cell markers. *Acta Biomater* **8**, 1440, 2012.
- Trappmann, B., Gautrot, J.E., Connelly, J.T., Strange, D.G., Li, Y., Oyen, M.L., *et al.* Extracellular-matrix tethering regulates stem-cell fate. *Nat Mater* **11**, 642, 2012.
- Pek, Y.S., Wan, A.C.A., and Ying, J.Y. The effect of matrix stiffness on mesenchymal stem cell differentiation in a 3D thixotropic gel. *Biomaterials* **31**, 385, 2010.
- Schmidt, C.E., Shastri, V.R., Vacanti, J.P., and Langer, R. Stimulation of neurite outgrowth using an electrically conducting polymer. *Proc Natl Acad Sci USA* **94**, 8948, 1997.
- Bolin, M.H., Svennersten, K., Wang, X.J., Chronakis, I.S., Richter-Dahlfors, A., Jager, E.W.H., *et al.* Nano-fiber scaffold electrodes based on PEDOT for cell stimulation. *Sens Actuators B Chem* **142**, 451, 2009.
- Del Valle, L.J., Aradilla, D., Oliver, R., Sepulcre, F., Gamez, A., Armelin, E., *et al.* Cellular adhesion and proliferation on poly(3,4-ethylenedioxythiophene): benefits in the electroactivity of the conducting polymer. *Eur Polym J* **43**, 2342, 2007.
- Gomez, N., Lee, J.Y., Nickels, J.D., and Schmidt, C.E. Micropatterned polypyrrole: a combination of electrical and topographical characteristics for the stimulation of cells. *Adv Funct Mater* **17**, 1645, 2007.
- Guimard, N.K., Gomez, N., and Schmidt, C.E. Conducting polymers in biomedical engineering. *Prog Polym Sci* **32**, 876, 2007.
- Abidian, M.R., Ludwig, K.A., Marzullo, T.C., Martin, D.C., and Kipke, D.R. Interfacing conducting polymer nanotubes with the central nervous system: chronic neural recording using poly(3,4-ethylenedioxythiophene) nanotubes. *Adv Mater* **2**, 3764, 2009.
- Xiao, Y.H., Martin, D.C., Cui, X.Y., and Shenai, M. Surface modification of neural probes with conducting polymer poly(hydroxymethylated-3,4-ethylenedioxythiophene) and its biocompatibility. *Appl Biochem Biotechnol* **128**, 117, 2006.
- Kim, D.H., Lu, N.S., Ghaffari, R., Kim, Y.S., Lee, S.P., Xu, L.Z., *et al.* Materials for multifunctional balloon catheters

- with capabilities in cardiac electrophysiological mapping and ablation therapy. *Nat Mater* **10**, 316, 2011.
26. George, P.M., Lyckman, A.W., LaVan, D.A., Hegde, A., Leung, Y., Avasare, R., *et al.* Fabrication and biocompatibility of polypyrrole implants suitable for neural prosthetics. *Biomaterials* **26**, 3511, 2005.
  27. Kim, D.H., Richardson-Burns, S.M., Hendricks, J.L., Sequera, C., and Martin, D.C. Effect of immobilized nerve growth factor on conductive polymers: electrical properties and cellular response. *Adv Funct Mater* **17**, 79, 2007.
  28. Christopherson, G.T., Song, H., and Mao, H-Q. The influence of fiber diameter of electrospun substrates on neural stem cell differentiation and proliferation. *Biomaterials* **30**, 556, 2009.
  29. Recknor, J.B., Sakaguchi, D.S., and Mallapragada, S.K. Directed growth and selective differentiation of neural progenitor cells on micropatterned polymer substrates. *Biomaterials* **27**, 4098, 2006.
  30. Georges, P.C., Miller, W.J., Meaney, D.F., Sawyer, E.S., and Janmey, P.A. Matrices with compliance comparable to that of brain tissue select neuronal over glial growth in mixed cortical cultures. *Biophys J* **90**, 3012, 2006.
  31. Saha, K., Keung, A.J., Irwin, E.F., Li, Y., Little, L., Schaffer, D.V., *et al.* Substrate modulus directs neural stem cell behavior. *Biophys J* **95**, 4426, 2008.
  32. Teixeira, A.I., Ilkhanizadeh, S., Wigenius, J.A., Duckworth, J.K., Inghanas, O., and Hermanson, O. The promotion of neuronal maturation on soft substrates. *Biomaterials* **30**, 4567, 2009.
  33. Ayala, R., Zhang, C., Yang, D., Hwang, Y., Aung, A., Shroff, S.S., *et al.* Engineering the cell-material interface for controlling stem cell adhesion, migration, and differentiation. *Biomaterials* **32**, 3700, 2011.
  34. Kotwal, A., and Schmidt, C.E. Electrical stimulation alters protein adsorption and nerve cell interactions with electrically conducting biomaterials. *Biomaterials* **22**, 1055, 2001.
  35. Wong, J.Y., Langer, R., and Ingber, D.E. Electrically conducting polymers can noninvasively control the shape and growth of mammalian cells. *Proc Natl Acad Sci USA* **91**, 3201, 1994.
  36. Lord, M.S., Foss, M., and Besenbacher, F. Influence of nanoscale surface topography on protein adsorption and cellular response. *Nano Today* **5**, 66, 2010.
  37. Vijay, V., Rao, A.D., and Narayan, K.S. *In situ* studies of strain dependent transport properties of conducting polymers on elastomeric substrates. *J Appl Phys* **109**, 084525, 2011.
  38. Bain, G., Kitchens, D., Yao, M., Huettner, J.E., and Gottlieb, D.I. Embryonic stem cells express neuronal properties in vitro. *Dev Biol* **168**, 342, 1995.
  39. Jagatha, B., Divya, M.S., Sanalkumar, R., Indulekha, C.L., Vidyand, S., Divya, T.S., *et al.* *In vitro* differentiation of retinal ganglion-like cells from embryonic stem cell derived neural progenitors. *Biochem Biophys Res Commun* **380**, 230, 2009.
  40. Kaufman, D.L., Houser, C.R., and Tobin, A.J. Two forms of the gamma-aminobutyric acid synthetic enzyme glutamate decarboxylase have distinct intraneuronal distributions and cofactor interactions. *J Neurochem* **56**, 720, 1991.
  41. Geppert, M., Goda, Y., Hammer, R.E., Li, C., Rosahl, T.W., Stevens, C.F., *et al.* Synaptotagmin I: a major Ca<sup>2+</sup> sensor for transmitter release at a central synapse. *Cell* **79**, 717, 1994.
  42. Longair, M.H., Baker, D.A., and Armstrong, J.D. Simple Neurite Tracer: open source software for reconstruction, visualization and analysis of neuronal processes. *Bioinformatics* **27**, 2453, 2011.
  43. Abramoff, M.D., Magelhaes, P.J., and Ram, S.J. Image processing with ImageJ. *Biophotonics Int* **11**, 36, 2004.
  44. Schneider, C.A., Rasband, W.S., and Eliceiri, K.W. NIH Image to ImageJ: 25 years of image analysis. *Nat Methods* **9**, 671, 2012.
  45. Zhu, X., Mills, K.L., Peters, P.R., Bahng, J.H., Liu, E.H., Shim, J., *et al.* Fabrication of reconfigurable protein matrices by cracking. *Nat Mater* **4**, 403, 2005.
  46. Lipomi, D.J., Lee, J.A., Vosgueritchian, M., Tee, B.C.K., Bolander, J.A., and Bao, Z.A. Electronic properties of transparent conductive films of PEDOT:PSS on stretchable substrates. *Chem Mater* **24**, 373, 2012.
  47. McBeath, R., Pirone, D.M., Nelson, C.M., Bhadriraju, K., and Chen, C.S. Cell shape, cytoskeletal tension, and rhoA regulate stem cell lineage commitment. *Dev Cell* **6**, 483, 2004.
  48. Discher, D.E., Janmey, P., and Wang, Y.L. Tissue cells feel and respond to the stiffness of their substrate. *Science* **310**, 1139, 2005.
  49. Eyckmans, J., Boudou, T., Yu, X., and Chen, C.S. A Hitchhiker's guide to mechanobiology. *Dev Cell* **21**, 35, 2011.
  50. Poon, B.C., Dias, P., Ansems, P., Chum, S.P., Hiltner, A., and Baer, E. Structure and deformation of an elastomeric propylene-ethylene copolymer. *J Appl Polym Sci* **10**, 489, 2007.

Address correspondence to:

K.S. Narayan, PhD

Molecular Electronics Laboratory

Chemistry and Physics of Materials Unit

Jawaharlal Nehru Centre for Advanced Scientific Research

Bangalore 560064

India

E-mail: narayan@jncasr.ac.in

Jackson James, PhD

Neural Stem Cell Biology Lab

Neurobiology Division

Rajiv Gandhi Centre for Biotechnology

Trivandrum 695014

India

E-mail: jjames@rgcb.res.in

Received: October 22, 2012

Accepted: March 26, 2013

Online Publication Date: May 10, 2013